Demonstration and Evaluation of the Ka-Band Array Feed Compensation System on the 70-Meter Antenna at DSS 14

V. Vilnrotter[1] and D. Fort[2]

This article documents the results of experiments designed to verify the gravity-compensation and tracking performance of a novel seven-channel 32-GHz (Ka-band) array feed compensation system (AFCS) for the DSN's 70-m antennas. The AFCS (along with other proposed compensation systems) was installed on the spare holography cone that was placed temporarily on the 70-m antenna in place of the X-band K-band radar (XKR) cone, which has been removed for repairs. These experiments took place from November 1998 through February 1999 and consisted of both quasar and spacecraft observations. Compensation performance was characterized in terms of both antenna-efficiency improvement and total signal-to-noise ratio (SNR) gain, while simultaneous-tracking capability was demonstrated by means of a least-squares tracking algorithm. A combined system consisting of the AFCS together with a deformable flat plate (DFP), designed to refocus divergent rays back in the array, also was examined briefly at low elevations. The results indicate that a properly designed real-time compensation system regains most of the SNR lost to deformations at low elevations and has the potential for similar improvements at high elevations, although this remains to be demonstrated.

I. Introduction

The current plan for DSN evolution calls for the use of 32-GHz (Ka-band) frequencies on large DSN antennas to increase antenna gain and useful communications bandwidth over that of current 8-GHz (X-band) and 2-GHz (S-band) systems, with reduced sensitivity to plasma effects. However, there are a number of new problems associated with the use of higher carrier frequencies, including greater sensitivity to antenna deformations and misalignments and more stringent pointing requirements due to narrower antenna beamwidths. Deformations and misalignments become increasingly problematic on the DSN's 70-m antennas, which are subject to severe gravitational stress, thermal gradients, focusing and other time-varying subreflector problems, and vibrations induced by the mechanical drive-system and by wind.

As the antenna tracks the target source (whether it is a spacecraft or a radio source), time- and elevation-dependent loss components are introduced due to the Earth's rotation and due to the motion of the spacecraft, even in the absence of wind. The combination of these effects can lead to large losses from

[1] Communications Systems and Research Section.

[2] Tracking Systems and Applications Section.

pointing errors and time-varying misalignments. Fortunately, most of these losses can be recovered by means of a properly designed compensation and tracking system that extracts the relevant deformation and pointing information from the received signal in real time.

Real-time compensation for antenna deformations due to gravity, thermal effects, and wind, together with accurate closed-loop tracking on 70-m antennas, will provide the DSN with greatly enhanced Ka-band capabilities for future missions: 8- to 10-dB gains over X-band on the 70-m antennas and up to 6-dB gains over 34-m antennas are projected at Ka-band.

II. Historical Background

An accepted technique for recovering losses due to gravitational deformations, thermal distortion, and wind is by means of a real-time compensation system employing an array of feeds in the focal plane. The potential use of feed arrays for real-time compensation of antenna distortions and pointing applications has been extensively addressed in the literature starting as early as 1970 [1–4].

A seven-element focal-plane array feed compensation system designed to recover gravitational and thermal losses on large DSN antennas has been constructed at the Jet Propulsion Laboratory and evaluated at the Goldstone complex. This system, called the array feed compensation system (AFCS), was developed to demonstrate real-time gravity compensation and closed-loop tracking of both spacecraft and radio sources at Ka-band frequencies. Both of these concepts have been successfully demonstrated in the pedestal room of the 34-m beam-waveguide antenna at DSS 13 between 1995 and 1998, using spacecraft—the Summer Undergraduate Research Fellowship Satellite (SURFSAT) and Mars Global Surveyor (MGS)—as well as radio sources (planets and quasars). These initial concept demonstrations on the 34-m antenna were followed by experiments on the 70-m antenna at DSS 14, including joint AFCS-plus-deformable flat plate (DFP) demonstrations on the 70-m antenna. In this experiment, the DFP functioned as a controllable RF reflector surface placed in front of the AFCS in order to refocus divergent RF fields into the array.

Compensation and tracking on the 70-m antenna are much more challenging than on 34-m antennas, due to greater gravitational deformations and greater vulnerability to thermal gradients and wind. Following successful compensation and tracking demonstrations on the 34-m beam-waveguide antenna at DSS 13, the AFCS was moved to DSS 14 and installed on the X-band K-band radar (XKR) cone of the 70-m antenna for experimental testing and demonstrations; later, the XKR cone was removed for upgrades, during which time the AFCS, the DFP, and a 12-GHz (Ku-band) holography receiver were installed in the refurbished holography cone, which then was mounted on the 70-m antenna in place of the XKR cone. For the following 3 1/2 months (from mid-November through February), a series of experiments (called the holography-cone experiments) was carried out to demonstrate and evaluate various candidate Ka-band gravity-compensation and tracking systems proposed for the DSN. Here we concentrate on the AFCS results but also describe the joint AFCS–DFP experiment carried out the last day, before the holography cone was removed.

III. Theoretical Background

The recently concluded holography-cone experiments attempted to characterize, evaluate, and compare candidate breadboard systems designed to improve Ka-band performance of the DSN's 70-m antennas by means of active gravity compensation and closed-loop tracking. Both the AFCS and the DFP were tested separately at virtually all elevations of interest (from 6- to nearly 85-deg elevation); in addition, these two systems also were tested jointly on DOY 056, where the role of the DFP was to refocus divergent rays back into the array, while the AFCS combined the collected signal fields optimally in order to maximize the received signal-to-noise ratio (SNR) in real time.

Due to severe time constraints, only the lower range of elevations could be investigated with the joint configuration, covering elevations from slightly above the rigging angle (about 50-deg elevation) down to nearly the software limit of the antenna (8.5 deg). Analysis of these data demonstrated that a joint Ka-band AFCS–DFP compensation system working together in real time could recover virtually all of the signal energy lost to gravitational deformation at intermediate to low elevations, effectively synthesizing an undistorted 70-m antenna at Ka-band frequencies.

In order to meet operational requirements, a practical gravity compensation system (such as the AFCS or a joint AFCS–DFP system) needs to perform two distinct tasks simultaneously: dynamic compensation for deformations due to gravity, thermal gradients, and wind, and real-time estimation of the best pointing offset in order to maximize the combined SNR. The details of these operations are discussed in greater detail in the following sections.

A. Deformation Compensation

The DSN's 70-m antennas originally were designed to receive 2-GHz (S-band) frequencies and later expanded and improved to enable efficient reception of 8-GHz (X-band) frequencies. At these relatively long wavelengths, structural deformations did not create a serious problem. However, at the much shorter Ka-band (32-GHz) wavelengths planned for the future, deformations of the antenna structure due to gravity, thermal gradients, and wind lead to unacceptable losses, particularly at very high and very low elevations. It has been found experimentally that, with conventional single-horn Ka-band receivers, SNR losses on the 70-m antenna at DSS 14 are approximately 4 dB at the lowest elevations and can exceed 6 dB at elevations above 80 deg, relative to the antenna's peak response. These losses must be greatly reduced before 70-m antennas can be usefully employed for operational reception of Ka-band signals.

The theoretical framework for optimal real-time combining of signals from several different horns in order to recover SNR has been detailed in several articles [5–7]. It has been shown that, for a given signal vector and arbitrary noise variance in each channel, the combining weights that maximize the SNR of the combined channel are given by the expression

$$\tilde{w}_k = \frac{\tilde{S}_k^*}{\sigma_k^2} \tag{1}$$

where $\tilde{S}_k$ is the signal amplitude in the kth channel, σ_k^2 is the variance of the noise, a tilde denotes a complex quantity, and an asterisk refers to complex conjugation. The optimally weighted combined digital signal samples can be expressed as

$$\tilde{z}(i) = \sum_{k=1}^{K} \tilde{r}_k(i)\tilde{w}_k \tag{2}$$

where the received noisy samples are $\tilde{r}_k(i) = \tilde{s}_k(i) + \tilde{n}_k(i)$ and the index i refers to time. The signal-to-noise ratio of the combined sequence, denoted as SNR_c, is defined as the average power in the weighted signal divided by the average power of the weighted noise:

$$\mathrm{SNR}_c = \frac{\left| \sum\limits_{k=1}^{K} \tilde{S}_k \tilde{w}_k \right|^2}{\sum\limits_{k=1}^{K} |\tilde{w}_k|^2 \sigma_k^2} = \sum_{k=1}^{K} \frac{\left|\tilde{S}_k\right|^2}{\sigma_k^2} \tag{3}$$

This expression shows that the SNR of the optimally combined signals is equal to the sum of the individual channel SNRs. Inherent in this result is the assumption that the combining weights are known exactly, a condition that typically cannot be achieved in practice since the combining weights must be estimated from imperfect real-time measurements of signal and noise parameters. However, when observing strong and stable Ka-band signals, the combining weights generally can be determined with sufficient accuracy to validate the assumption of perfect weight estimates. Alternatively, a straightforward approach to determining the SNR of the combined channel is to measure it directly from the combined samples; both of these approaches were employed simultaneously by the AFCS digital signal-processing assembly to help confirm the accuracy of the measurements.

B. Antenna Pointing and Tracking

Functional requirements typically are very different for collecting experimental data and for operational reception of spacecraft telemetry. Experimental data are collected using a closed-loop boresighting algorithm; this is a direct-measurement algorithm that determines the direction to the peak of the gain pattern by measuring the signal power at several points near the peak and interpolating the results. This approach is well understood and yields accurate results when performed under stable observing conditions but requires serial measurements of off-source points to trace out the power distribution and, hence, introduces an inherent SNR variation into the signal. While this is acceptable for experimental data gathering, it is not desirable for telemetry reception, when unwanted SNR variations degrade the decoding of the data. In addition, the serial nature of the measurements can lead to pointing errors if there is significant temporal variation in the spacecraft power, as often happens during orbital maneuvers. For these reasons, the array-feed inferred-measurement tracking algorithm is preferred for operational use, since this algorithm automatically determines the best pointing direction from simultaneous measurements of the signal.

The inferred-measurement tracking algorithm performs simultaneous measurements of the signal in all seven array-feed channels, without ever pointing the antenna off-source, as must be done with conventional boresighting or conical-scanning (CONSCAN) techniques. Although this tracking algorithm could not be fully demonstrated during the recently concluded holography-cone experiments due to lack of time, very high-quality data were obtained from the Deep Space One (DS1) spacecraft that can be used to develop and improve the tracking algorithm and simulate its performance on the real antenna.

IV. AFCS Design

A block diagram of the array feed compensation system (AFCS) used in the recently concluded holography-cone experiments is shown in Fig. 1. This system essentially is identical to the one evaluated on the XKR cone of the 70-m antenna at DSS 14 and previously in the pedestal room of the 34-m antenna at DSS 13. The entire system can be conveniently separated into two major sections: an analog front end (AFE) and a digital signal-processing assembly (DSPA). The AFE consists of a seven-horn feed array, cryogenically cooled high-electron mobility transistor (HEMT) low-noise amplifiers (LNAs), and a seven-channel downconverter assembly that translates the received signal from Ka-band to nominal 300-MHz intermediate frequency (IF). The DSPA further downconverts the IF signal to complex baseband, where it is sampled and combined, using real-time estimates to compute the optimum combining weights. Digital algorithms are employed to extract the pointing information from the signal, which then can be used to keep the antenna pointed on-source.

A. Array-Feed Front End

The feed array consists of seven identical smooth-walled Potter horns, each 1 3/4 inches in diameter, providing 22-dBi of gain at 32 GHz. The wall of each horn is tapered near the top to facilitate close packing, thus minimizing the loss of signal energy between the horns. The cryogenic front end contains

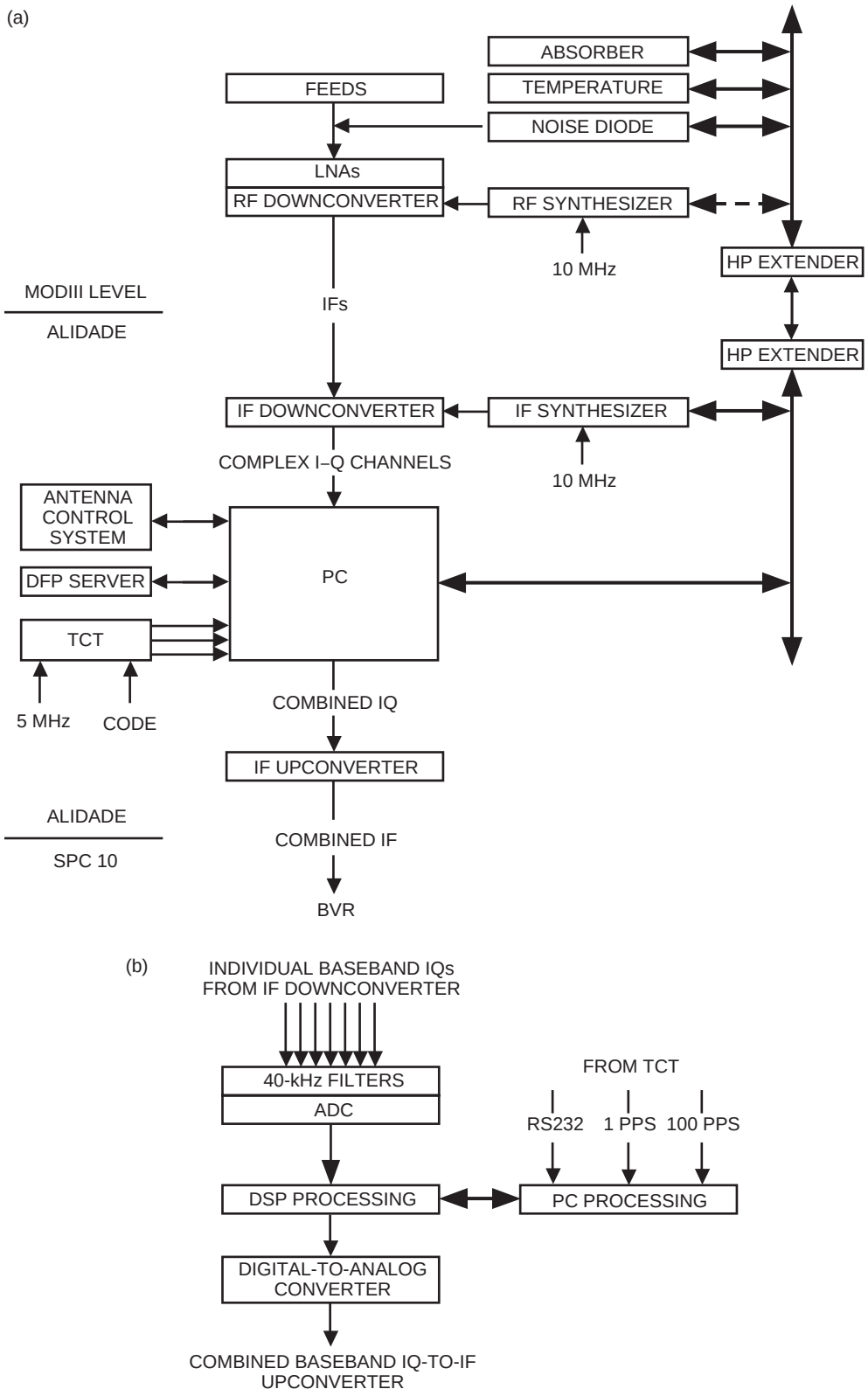

Fig. 1. The AFCS: (a) block diagram and (b) DSPA (resides in the PC).

circular-to-rectangular waveguide transitions; polarizers; 20-dB couplers for each channel to enable external noise diode and tone inputs for calibration; three-stage HEMT LNAs that provide nominally 25 dBi of gain, thus establishing high SNR without adding significant receiver noise to the signal; and thermal components such as a heat sink and a charcoal trap to gather up the remaining molecules and, thus, help produce a better vacuum. The output of each HEMT LNA is an amplified RF signal at a nominal center frequency of 32 GHz. Next, the seven RF signals are translated to 300-MHz IF by the seven-channel downconverter assembly and transmitted via seven coaxial IF cables to the DSPA, located in the alidade of the 70-m antenna.

In the alidade, the seven IF signals are processed by an IF-to-baseband downconverter assembly, which shifts the signals from 300 MHz (nominal center frequency) to a video frequency within the passband of the digital system. Both in-phase (I) and quadrature-phase (Q) components are extracted from the IF signals, downconverted to a baseband video center frequency of approximately +20 kHz (default, manually resettable), sampled using a bank of 14 analog-to-digital converters (ADCs), and thus converted to complex digital samples. From this point on, the digital processing depends on the type of source being observed. The DSPA has been designed to process either broadband sources (radio sources such as quasars and planets) or narrowband sources, such as those produced by the residual carrier of a Ka-band spacecraft. Either approach can be selected by the user; in each case, the final result is a combined-channel output with maximized SNR, although different techniques must be employed to estimate the optimum combining weights for the two cases. In addition, the DSPA also extracts pointing information from the complex baseband samples, thus providing an option to update the antenna's predict-driven blind-pointing algorithm with closed-loop tracking based on real-time pointing information; the user can choose between broadband and narrowband versions of an accurate and well tested AFCS boresighting algorithm or the experimental inferred-measurement tracking algorithm described above.

B. Digital Signal-Processing Assembly (DSPA)

The DSPA uses four TMS320C40 floating point digital signal processors (DSPs) operating at 50 MHz and connected in a circular chain, located on signal-processing boards within the PC. The incoming data are sampled continuously with 16-bit resolution at 96,000 samples per second and stored in 750-sample buffers by the first processor, then shifted from processor to processor until finally the combined data are added into the buffer. The first processor then sends the combined channel samples to the digital-to-analog converters. The second processor removes any DC offsets from the samples and scales the data using parameters sent by the PC. The third processor produces the combined-channel samples using complex weights obtained from the PC and puts the result in the buffer as the eighth channel. The fourth DSP processes all eight feeds, as instructed by the PC, and sends the results (8 complex numbers) to the PC for additional processing or for output 128 times a second (note that $128 \times 750 = 96,000$). The operations performed by the fourth processor on demand are

(1) Return the first sample in the buffer—used for diagnostic purposes

(2) Return the sum of all samples—used for calibrating DC offsets

(3) Return the sum of squares of all samples—used for power measurements

(4) Return the cross-correlation of each channel with the central channel—used for calculating combining weights for broadband sources (quasars)

(5) Return the sum of the samples rotated by a phase model supplied by the PC—used for calculating the weights for narrowband sources (spacecraft)

The PC is used for both control and data processing and incorporates a real-time operating system (RT-KERNEL). Data processing includes reading time from the time code translator (TCT) and responding to 1-pulse-per-second (PPS) and 100-PPS interrupts generated by the TCT. DC offsets and gains are calculated and sent to the DSPA when requested by the user (these offsets and gains change very slowly,

if at all). When observing spacecraft, carrier-frequency predicts are generated from predict files, and the carrier frequency is sent to the DSPA 128 times a second. Correlation and rotation results are used to derive the complex weights via a Fourier transform technique and downloaded to the DSPA periodically. The power measurements also are used to perform conventional system calibrations with a noise diode and absorber.

V. Efficiency Measurements

Single-horn antenna-efficiency measurements were carried out using the central channel of the AFCS. These were based on simultaneous power measurements of the Ka-band calibrator 3C274 using (1) the digital power meter incorporated into the DSPA and (2) analog power measurements using a calibrated Hewlett Packard (HP) power meter connected directly to the IF of the central channel. Source power was measured on three separate occasions near the rigging angle under good atmospheric conditions (clear, calm weather); the power readings were averaged, and the average elevation of the three measurements was computed. Antenna efficiency at each elevation was estimated by dividing the average temperature of the source, T_{src}, by the published value[3] for 3C274 for a 100 percent efficient antenna, $T_a = 11.9$ kelvins. The results of these measurements are as follows:

DOY	Elevation, deg	T_{src}, K	Efficiency, percent
011	45	3.8	31.9
035	41	3.1	26.1
038	45.4	3.6	30.4

The average efficiency was found to be 29.4 percent at an average elevation of 43.8 deg.

The source power was also measured simultaneously using digital techniques and compared with the HP measurements, which were taken as the reference. The scale factors thus derived were transferred to the digital-power measurements of other radio sources, namely 3C273 and 3C84, when these sources were near the rigging angle. Thus, an estimate of antenna efficiency as a function of elevation was obtained over an elevation range of 6 to 84 deg. Since the power in all seven channels was recorded by the DSPA on every track, this information was also used to measure the efficiency improvement provided by the array (the combined-channel data in Fig. 2).

Analysis of the fourth-order polynomial fit to the central-channel data in Fig. 2 indicates that, at very low elevations (near 6 deg), the central-channel efficiency drops to about 11 percent, representing an efficiency loss of 4.3 dB, while, at very high elevations (84 deg), the measured efficiency drops to 7 percent, representing a loss of 6.2 dB from the peak response. Similarly, analysis of the fourth-order fit to the combined-channel data indicates a peak response of 36 percent near 42-deg elevation, with low- and high-elevation efficiencies of 17 percent, representing losses of 3.25 dB at the extreme elevations. Note that these data have not been corrected for atmospheric extinction, which is most prominent at low elevations; using the measured value for zenith extinction of 0.1 dB (corresponding to 1 air mass), the correction for lower elevations can be found by determining the number of air masses at the elevation of interest. The attenuation at 6-deg elevation is approximately 1 dB, or a factor of 1.25; hence, both central- and combined-channel efficiencies should be increased by this amount, yielding 13.7 and 21.2 percent, respectively, for the corrected central- and combined-channel efficiencies. Ignoring the small correction

[3] P. Richter, *Radio Source List for Antenna Calibration*, JPL D-3801 (internal document), DSN 890-269, Jet Propulsion Laboratory, Pasadena, California, October 15, 1994.

due to the slight increase in air mass at the rigging angle and above, this implies that the corrected efficiency loss for the central channel at 6-deg elevation is 3.3 dB, while that of the corrected combined channel is 2.3 dB. Taking the ratios of combined-to-central channel efficiencies, the combining gains estimated from these data are 1.9, 0.87, and 3.8 dB at 6, 42, and 84 deg, respectively.

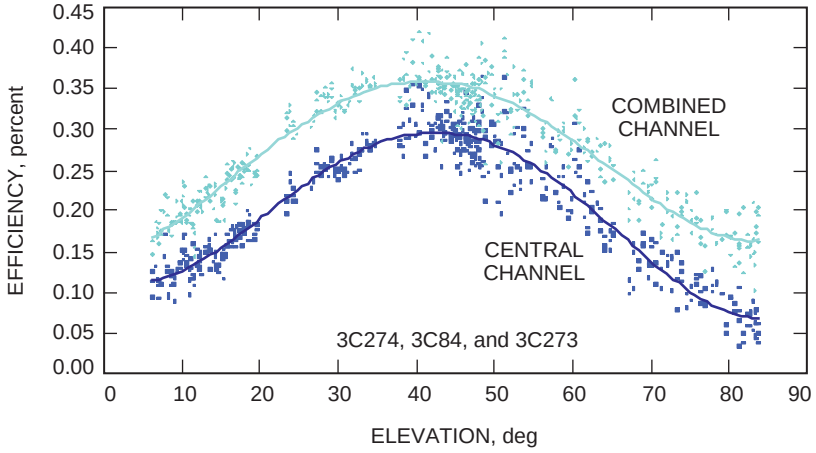

Fig. 2. Efficiency curve of the 70-m antenna: AFCS central and combined channels (not corrected for atmospheric effects).

VI. Array Feed Compensation System

A. Combining

The New Millennium spacecraft DS1 provided a stable Ka-band signal throughout the holography-cone experiments. After its Ka-band transmitter was turned on, DS1 produced a strong Ka-band signal that usually contained a significant residual-carrier component whose power depended on the modulation index. There were two modes of operation for the Ka-band downlink: one-way and two-way modes. In the one-way mode, the spacecraft's onboard oscillator was used to generate the carrier signal while, in two-way mode, a highly stable frequency reference was transmitted up to the spacecraft from the ground, which the spacecraft oscillator used as reference, modulated, and retransmitted to the ground.

A typical DS1 data-gathering track consisted of the following steps: (1) frequency and pointing predicts were obtained and supplied to Signal Processing Center (SPC) 10; (2) the antenna was blind pointed toward the spacecraft, and the frequency predicts were used to acquire the residual carrier; (3) the residual carrier was downconverted into the passband of the DSPA (nominally 20 kHz), integration time and loop gain were set (a minimum 1-second integration time with the current architecture), and the frequency-tracking loops were locked up; (4) a boresighting sequence was initiated to refine antenna pointing in order to peak up the signal; and (5) data gathering or other pertinent experiments commenced.

During a typical DS1 track, most of the time was allocated to collecting combining data over a range of elevations. Since the antenna tends to exhibit considerable drift from the pointing model (particularly at low and high elevations), it was necessary to update the antenna pointing in real time; this was accomplished using the coherent version of the array-feed boresighting algorithm. The array-feed boresighting algorithm applies small positive and negative pointing offsets from the nominal on-source direction along both the elevation and cross-elevation axes, measures the signal power at each offset (including the nominal on-source direction), and estimates the direction to the peak from a quadratic fit to the data. The algorithm records the complex signal voltage at the end of each integration time, measures the rms noise voltage, and updates the optimum combining weights in all seven channels. It also measures and records the complex signal voltage and rms noise voltage in the optimally combined channel. This information

can be used to determine the SNR in the combined channel directly. Dividing the SNR of the combined channel by the SNR of the central channel yields the combining gain, G_c, of the AFCS, formally defined as

$$G_c \equiv \frac{\text{SNR of combined channel}}{\text{SNR of central channel}} \tag{4}$$

Data collected on DOY 038 are displayed in two different ways in Figs. 3(a) and 3(b): the first shows signal power as a function of elevation on a linear scale to facilitate comparison with the efficiency curve of Fig. 2, while the second shows SNR (in dB) as a function of time. The compensating effect of the AFCS is most clearly demonstrated in Fig. 3(b), where the SNR loss at high elevation, as the antenna tracks the source through transit, is significantly less in the combined channel than in the central channel; at high elevations, the combining gain is seen to be approximately 3 dB, yielding a less severe SNR loss than in the uncompensated central channel.

Combining gain was found to be a useful quantity for evaluating AFCS performance since it is not affected by perturbations common to all seven channels at the same time. For example, it was found that the relatively long, 1-second integration time employed by the current DSPA architecture produced an effective frequency-tracking-loop bandwidth that was too narrow to track the phase dynamics of the received signal accurately, occasionally resulting in simultaneous signal fades in all seven channels. This

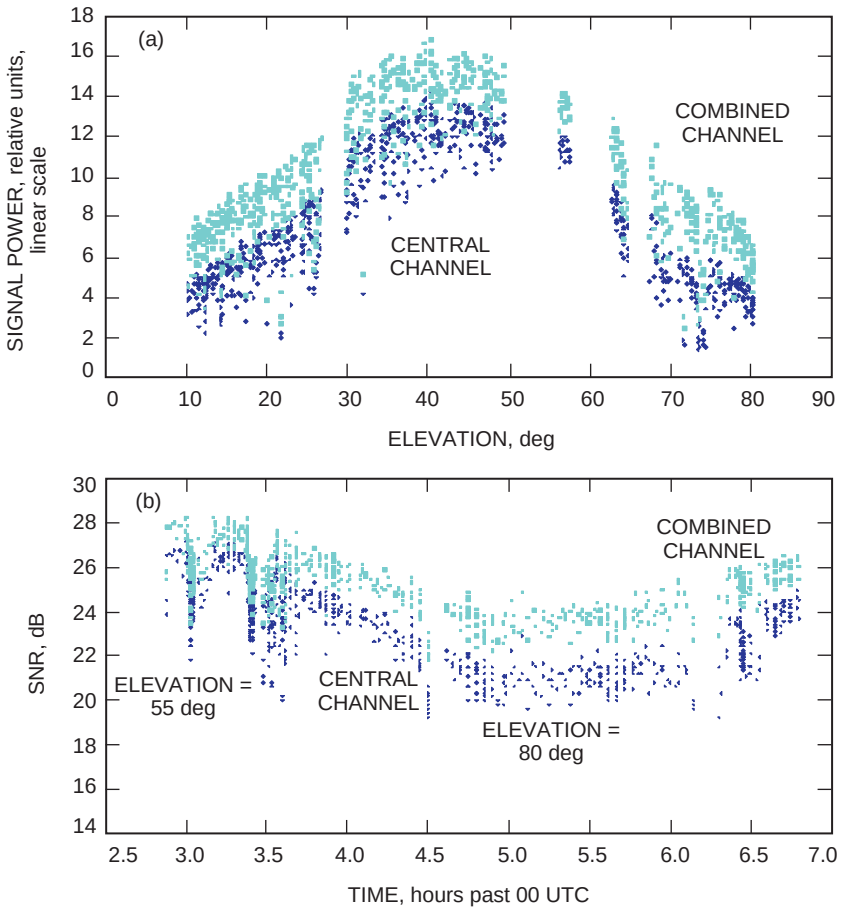

Fig. 3. AFCS track of DS1 on DOY 038: (a) signal power as a function of elevation and (b) SNR as a function of time.

caused large scatter in the SNR of each channel as well as of the combined channel, as is evident in Figs. 3(a) and 3(b). However, since the random fading coefficients were identical in both the combined and central channels, taking their ratio as in Eq. (4) led to cancellation of the fade coefficients regardless of their instantaneous value, resulting in much less scatter in the combining-gain estimates.

The improvement in the combining-gain data is clearly illustrated in Fig. 4, where the data exhibit much less scatter than the original SNR data. Note that, above 60-deg elevation, the data appear to split into two distinct branches, indicating an azimuth dependence in the combining gain; the upper branch corresponds to the ascending part of the track (before transit) while the lower branch corresponds to descent toward the horizon (after transit). This somewhat asymmetrical behavior of the antenna has been observed on all occasions, but the exact cause is not well understood at this time.

Consistent with previous analyses of both radio sources and DS1 data, the combining gain at low elevations is seen to approach 2 dB, dropping to less than 1 dB near the rigging angle, and increasing to as much as 4 dB around 75 deg ascending, 3 dB near transit, and a little over 2 dB around 75 deg descending. The third-order trend line indicates average gain at a given elevation, without taking into account the azimuth dependence of the gain curve at the high elevations. It should be emphasized that all of the above data were obtained using the array-feed boresighting algorithm, which maximizes the power in the central channel but does not necessarily maximize the SNR in the combined channel. It follows, therefore, that even higher combining gains can be achieved with a pointing algorithm that is designed to maximize the SNR in the combined channel, although these improvements remain to be quantified.

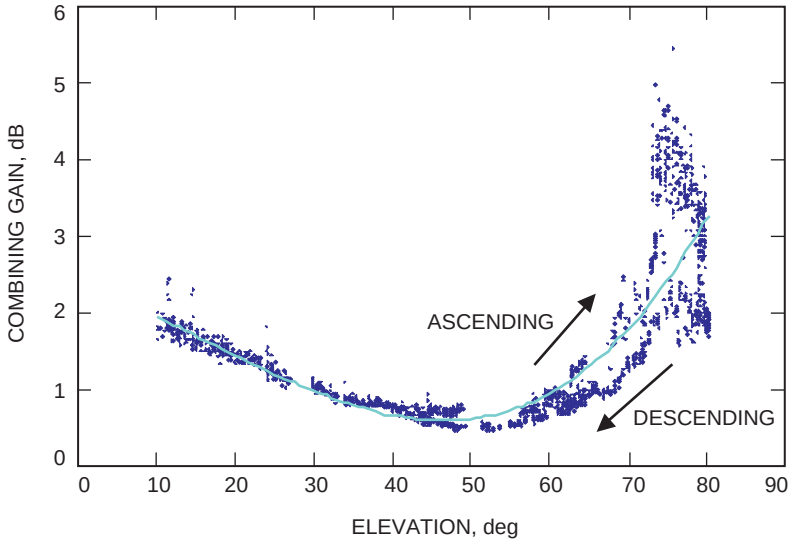

Fig. 4. Array-feed combining gain as a function of elevation.

B. Tracking

A very accurate direct-measurement boresighting algorithm that works with broadband sources as well as coherent tones has been developed and installed into the AFCS before the start of the holography-cone experiments and has been used throughout to provide closed-loop pointing of the antenna. This algorithm relies on the periodic introduction of small pointing offsets to estimate the direction of the signal peak, which unfortunately results in unavoidable SNR loss when the antenna is pointing off-source. In addition, the inherent serial nature of the measurements makes them vulnerable to errors due to variations in signal power or changes in atmospheric conditions during the measurements. The inferred-measurement algorithm currently being developed uses simultaneous measurements of the signal in all seven channels, without the need to point the antenna off-source; thus, it is immune to signal-power variations and does not degrade the SNR of the signal. Due to time constraints, all of the tasks proposed

in the original experiment plan could not be addressed; in particular, the development and demonstration of the inferred-measurement algorithm could not be completed. However, very high quality data were obtained from tracking the DS1 spacecraft, which was near the Earth during these experiments and, therefore, provided a strong and stable signal.

Since the feed array can be viewed as an instrument for obtaining samples of the focal-plane field distribution, it should be possible to extract accurate pointing information from these samples in real time, even in the presence of antenna distortions. This hypothesis was tested during the holography-cone experiments by measuring and recording the complex array response for a raster of small offsets from the optimum pointing direction at 10-deg elevation increments while tracking DS1. The raster model thus compiled effectively characterized the effects of antenna distortion at all elevations and simultaneously provided a means for determining the inherent pointing resolution of the feed array on the 70-m antenna. It was concluded that 1-mdeg pointing offsets were detectable at all elevations despite antenna distortion, implying that with additional interpolation and refinements this technique can provide real-time pointing updates with less than 1-mdeg uncertainty.

Due to lack of time, only a relatively simple, coarse-quantized least-squares tracking algorithm could be installed into the DFPA in order to provide initial information about AFCS inferred-measurement tracking capabilities under actual operating conditions. This least-squares algorithm tested the real-time observables at 2-mdeg increments in elevation and cross-elevation and did not employ interpolation to refine its estimates; therefore, it could not be used to fully demonstrate the inherent tracking accuracy of the AFCS. However, recovery from applied offsets and closed-loop tracking was verified on DOYs 037 and 038, at elevations of 46, 57 and 73 deg, while tracking DS1. In each case, the least squares inferred-measurement algorithm found a stable point, and continued to track the source close to the true peak (with approximately a 2-mdeg offset in some cases, as expected due to the rough quantization). Finer quantization in the model and the use of interpolation will reduce these algorithm offsets to less than 1 mdeg in future versions.

An example of AFCS recovery and tracking by means of the inferred-measurement least-squares tracking algorithm is provided in Fig. 5, which is part of the record of the track on DOY 037, at an elevation of 46 deg. The time axis is in hours past 00 UTC. The AFCS was tracking DS1 using the least-squares tracking algorithm, registering a 40 dB-Hz SNR in the central channel and about 41 dB-Hz in the combined channel; at approximately 1.885 hours UTC, the tracking algorithm was stopped and offsets of +6 mdeg in both elevation and cross-elevation were applied, causing a 15-dB loss in the central channel and a 5-dB loss in the combined channel. After reactivation, the least-squares algorithm measured the applied offsets (with 2-mdeg resolution) and correctly repointed the antenna toward the source, clearly demonstrating SNR recovery. This test was repeated at about 1.915 UTC, this time with ± 6 mdeg offsets, with similarly successful results. Additional tracking experiments carried out on DOY 038 at elevations as high as 73 deg also were successful, demonstrating the ability of this AFCS inferred-measurement algorithm to keep the antenna pointed on-source, even in the presence of severe antenna distortions.

VII. Joint AFCS–DFP Measurements

Due to time constraints on the holography-cone experiments, only the lower range of elevations could be investigated with the joint AFCS–DFP configuration, covering elevations from slightly above the rigging angle (about 50-deg elevation) down to nearly the software limit of the antenna (8.5 deg). For this joint configuration, the AFCS front end was moved from its initial position on the focal circle looking directly at the subreflector (designated as F1) to a new location behind the DFP inside the cone (F2). Apparently, the vacuum seal on the dewar was slightly damaged during the move, because the dewar failed to cool down to cryogenic temperatures after it was moved. Following several attempts to cool the dewar, this effort was abandoned, and preparations were made to observe DS1 with a room-temperature system. Fortunately, due to the proximity of the spacecraft, room-temperature operation was a viable

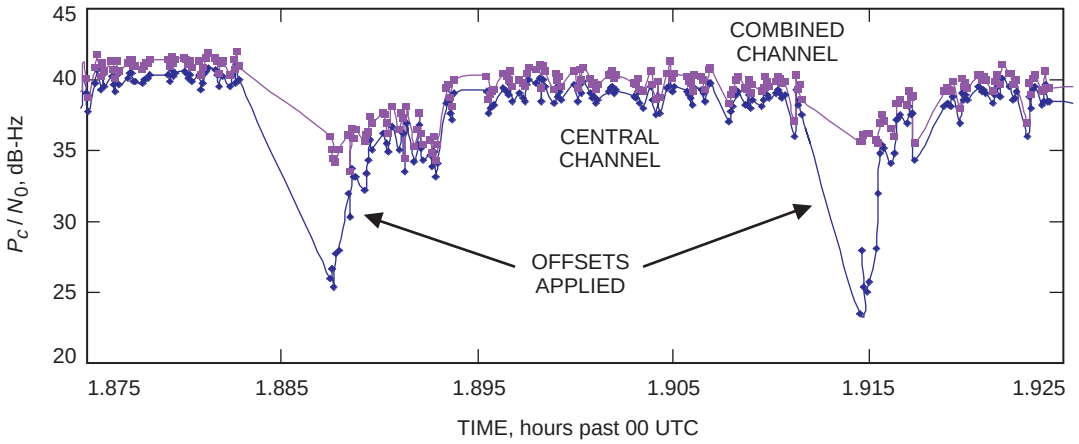

Fig. 5. Pointing recovery and tracking via the least-squares tracking algorithm.

option; the strong Ka-band residual carrier yielded SNRs in excess of 30 dB-Hz near the rigging angle even with room-temperature LNAs, which was more than adequate for conducting the joint AFCS–DFP compensation experiments.

Three distinct experiments were carried out on DOY 056 while tracking DS1: the peak response of each horn was mapped using direct boresights on each horn; the central and combined channels were supplied to a Block V Receiver (BVR) in SPC 10 for independent combining-gain measurements; and joint AFCS–DFP compensation experiments were carried out as the spacecraft descended toward the horizon. The results of these activities are summarized in the following sections.

A. Mapping of the Array-Feed Horns

The horn-mapping activity took place between 0324 UTC and 0411 UTC as the spacecraft continued to ascend from about 70- to 77-deg elevation. First, two boresights were performed on the central horn (channel 1), the offsets from the predicts noted (these offsets were needed to peak up the source in the new location on the cone), and a digital SNR measurement was made. The antenna then was repointed in the nominal direction of horn 2 and the source located in the second channel using a manual search. The signal then was peaked up using two more boresights on the output of the second horn, after which the SNR was recorded. This process was repeated for the remaining horns. Finally, the SNR of the central horn was remeasured as a consistency check. The results are summarized in Table 1. Note the 2-dB drop in the central-channel SNR between the first and last measurements as well as the change in the offsets due to the higher elevation of the last measurement.

B. Independent Verification of Combining Gain

During most of the holography-cone experiments, combining gain was measured digitally with the DFPA, using two nearly independent techniques: first, the SNR in each channel was measured and the sum of the channel SNRs computed to obtain an estimate of the combined-channel SNR as in Eq. (3); next, the actual SNR of the optimally weighted combined channel was measured after the estimated combining weights were applied. In each case, the resulting SNR was divided by the maximized SNR of the central channel to obtain the combining gain. The results of both measurements were recorded and displayed on the monitor on demand. Typically, both measurements agreed to within a few tenths of a dB, providing a degree of mutual confirmation, since fundamentally different measurement techniques were employed in the two cases.

In order to further check the validity of these digital measurements, each output channel (central and combined) was upconverted to 300-MHz IF, transmitted to SPC 10, and input to a BVR. The BVR

Table 1. Mapping the peak response of the seven array-feed horns.

Horn no.	Elevation, deg	Offsets, mdeg	SNR, dB
1	70	(−13.4, 2.6)	30.5
2	71	(−5.9, 12.5)	29.5
3	72	(−0.6, 1.6)	32.4
4	73	(−8.3, −8.9)	30.0
5	74	(−20.9, −6.3)	28.6
6	75	(−25.3, 4.6)	29.9
7	76	(−15.9, 14.5)	28.2
1	77	(−11.0, 4.4)	28.6

locked up to the residual carrier of either the central or the combined channel (whichever was selected for transmission) and recorded its own estimate of the signal-to-noise ratio. Since only a single-channel analog upconverter was available, it was decided to incorporate a digital switch into the DSPA, enabling selection of either the central or the combined channel. The baseband in-phase and quadrature-phase signals were supplied to the upconverter, which then produced a single (real) IF suitable for transmission to the BVR.

At an elevation of 78 deg descending, the output of the DSPA was switched between the central and combined channels, and the SNR measured by the BVR was recorded. The results of this verification experiment are shown in Fig. 6; it can be seen that the SNR of the combined channel is close to 29 dB-Hz throughout the experiment, while that of the central channel falls below 26 dB-Hz near the end, indicating a gain of up to 3 dB. These results are consistent with SNRs measured and recorded previously by the DSPA at similar elevations, as previously shown in Fig. 4.

C. Joint AFCS–DFP Combining Experiment

Analysis of the data obtained on DOY 056 clearly demonstrated that a joint Ka-band AFCS–DFP compensation system working together in real-time could recover virtually all of the signal energy lost to gravitational deformations at intermediate to low elevations, effectively synthesizing an undistorted 70-m antenna at Ka-band frequencies.

On DOY 056, DS1 was tracked continuously as it descended from an elevation of approximately 50 deg down to 8.5 deg. Both BVR and AFCS data were taken simultaneously during the track. With the DFP

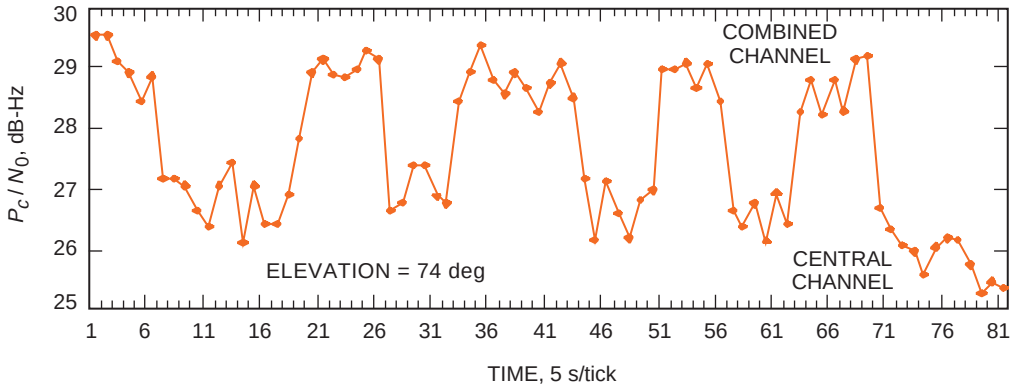

Fig. 6. BVR measurement of the AFCS central- and combined-channel SNR.

flat, boresights were performed to center the source in the central channel, after which the DFP was flexed in an attempt to refocus the distorted fields back into the array. Since the data recorded by the BVR are not elevation tagged, but only time-tagged, the operator's notes were used to help identify the state of the DFP; these "flat" and "flex" times were confirmed using recorded AFCS data, which contain both time and elevation information.

The AFCS data collected during this joint track are shown in Fig. 7(a), where all feed powers were normalized to the signal power in the central channel in order to eliminate the effects of possible variations in signal power. With equal noise power in all of the channels, SNR and signal power are proportional, hence the normalized power of the combined channel is recognized as the combining gain defined earlier in Eq. (4). Figure 7(b) is a logarithmic plot of the same data that better shows the contribution of the outer horns to the total collected signal power as a function of elevation.

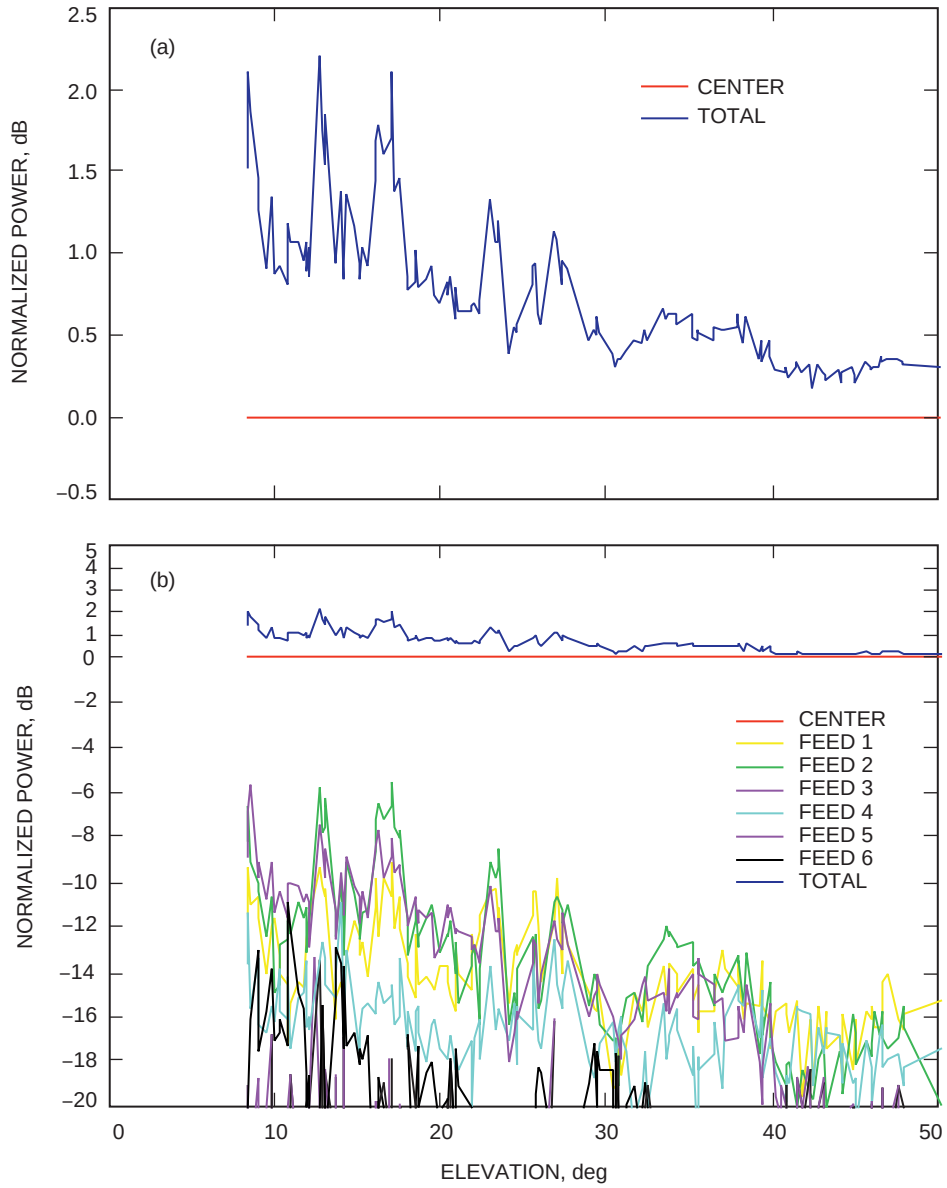

Fig. 7. AFCS data (a) taken during a DS1 track on DOY 056 (DFP flat and flexed) and (b) a logarithmic plot of the data in Fig. 7(a).

The normalized power in all of the outer feeds, as well as the total power, varies as the state of the DFP changes: when the DFP is flat, the outer feeds contain more power, and when the DFP is flexed, the power in the outer feeds is reduced, but not eliminated, as the DFP successfully concentrates some of the distorted signal fields into the central horn of the array. This effect can be seen clearly in Fig. 7(a) at elevations of 8.5, 13, 16.5, 23, 28, and 33 deg, becoming less pronounced at the higher elevations. At low elevations, the AFCS combining gain is approximately 2 dB when the DFP is flat, but tends to remain above 1 dB even as the DFP is flexed. Results based on analysis of the BVR data are presented in Table 2.

Table 2. Average combining gain of the AFCS, DFP, and AFCS Plus DFP on DOY 056.

Elevation, deg	G_{AFCS}, dB	G_{DFP}, dB	G_{joint}, dB	ΔAFCS, dB	ΔDFP, dB
8.5	2.1	1.8	2.9	1.1	0.8
13	1.8	1.6	2.5	0.9	0.7
16.5	1.6	1.4	2.2	0.8	0.6
23	1.2	1.1	1.8	0.7	0.6
28	1.1	0.9	1.5	0.6	0.4
33	0.75	0.6	1.0	0.4	0.25
38	0.5	0.3	0.6	0.3	0.1

The various gains used in Table 2 are defined as follows: $G_{\mathrm{AFCS}} = G_c$ is the array gain over the central channel, as defined in Eq. (4), when the DFP is flat; G_{DFP} is the increase in signal power in the central channel when the DFP is flexed; G_{joint} is the gain over the uncorrected central channel due to both the DFP and the AFCS operating jointly to recover SNR losses; ΔAFCS is the gain contributed by the AFCS to G_{joint}, over that of the DFP acting alone; and ΔDFP is the gain contributed by the DFP to G_{joint}, over that of the AFCS acting alone.

The results in Table 2 are also shown in graphical form in Fig. 8, where the measured AFCS gains (in dB) have been added to the SNR measurements recorded by the BVR. It can be concluded that either the AFCS or the DFP acting individually can recover up to 2 dB of SNR at low elevations; however, the combination of the two systems operating jointly yields substantial additional improvements, amounting to more than 1 dB over that of the DFP acting alone.

VIII. Summary and Conclusions

It has been demonstrated that most of the SNR (or efficiency) losses incurred from mechanical antenna distortions can be recovered by means of a properly designed real-time compensation system consisting of a seven-element array-feed receiver (AFCS) operating in combination with a deformable flat plate (DFP) designed to redirect divergent rays back into the array. It has been shown that such a combination system recovers approximately 3 dB out of a possible 4 dB at low elevations and is believed capable of recovering 5 dB out of more than 6 dB lost at high elevations, effectively synthesizing a flat antenna response at Ka-band frequencies. This approach has the added advantage of providing simultaneous closed-loop tracking by means of array-feed inferred-measurement tracking algorithms, one of which was successfully demonstrated during the holography-cone experiments.

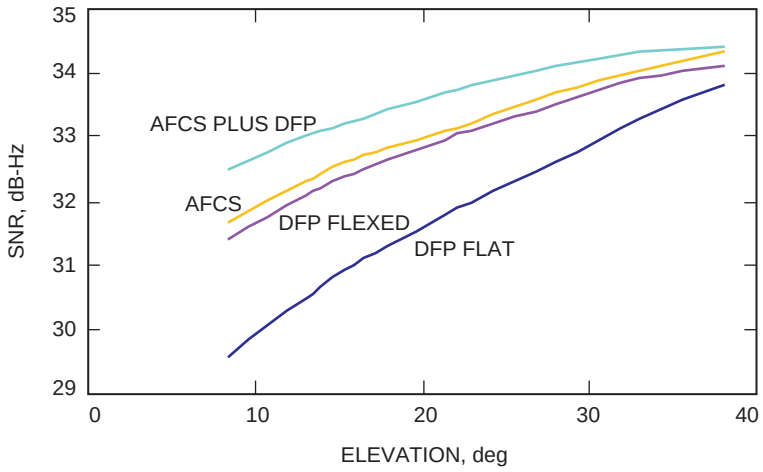

Fig. 8. Results of the joint AFCS-plus-DFP compensation experiment.

Acknowledgment

The authors would like to thank Vahraz Jamnejad for generating the plots in Figs. 7(a) and 7(b).

References

[1] A. W. Rudge and D. E. N. Davies, "Electronically Controllable Primary Feed for Profile Error Compensation of Large Parabolic Reflectors," *Proceedings of IEEE*, vol. 117, pp. 351–358, 1970.

[2] S. J. Blank and W. A. Imbriale, "Array Feed Synthesis for Correction of Reflector Distortion and Vernier Beamsteering," *The Telecommunications and Data Acquisition Progress Report 42-86, April–June 1986*, Jet Propulsion Laboratory, Pasadena, California, pp. 43–55, August 15, 1986.
http://tmo.jpl.nasa.gov/tmo/progress_report/42-86/86E.PDF

[3] A. R. Cherrete, R. J. Acosta, P. T. Lam, and S. W. Lee, "Compensation of Reflector Antenna Surface Distortion Using an Array Feed," *IEEE Transactions on Antennas and Propogation*, vol. 37, pp. 966–978, August 1989.

[4] P. W. Cramer, "Initial Studies of Array Feeds for the 70-Meter Antenna at 32 GHz," *The Telecommunications and Data Acquisition Progress Report 42-104, October–December 1990*, Jet Propulsion Laboratory, Pasadena, California, pp. 50–67, February 15, 1991.
http://tmo.jpl.nasa.gov/tmo/progress_report/42-104/104E.PDF

[5] V. Vilnrotter, E. Rodemich, and S. Dolinar, Jr., "Real-Time Combining of Residual Carrier Array Signals Using ML Weight Estimates," *IEEE Transactions on Communications*, vol. 40, pp. 604–615, April 1992.

[6] V. Vilnrotter, D. Fort, and B. Iijima, "Real-Time Array Feed System Demonstration at JPL," *Multifeed Systems for Radio Telescopes*, Astronomical Society of the Pacific Conference Series, vol. 75, pp. 61–73, 1995.

[7] K.-M. Cheung and V. Vilnrotter, "Channel Capacity of an Array System for Gaussian Channels With Applications to Combining and Noise Cancellation," *The Telecommunications and Data Acquisition Progress Report 42-124, October–December 1995*, Jet Propulsion Laboratory, Pasadena, California, pp. 53–62, February 15, 1996.
http://tmo.jpl.nasa.gov/tmo/progress_report/42-124/124D.pdf